



Microscopic study of electronic screening at simple metal surfaces  
by Jorge Alberto Gaspar

A thesis submitted in partial fulfillment of the requirements for the degree of Doctor of Philosophy in  
Physics

Montana State University

© Copyright by Jorge Alberto Gaspar (1991)

Abstract:

We study electronic screening processes at simple metal surfaces. The jellium model is used for the ionic background of the metal. The linear electronic response of the metal is computed within the local density approximation of density functional theory. This theory is applied to two specific problems: 1) the electronic response of an alkali-metal overlayer chemisorbed on aluminum, and (2) the spectrum of surface vibrations of aluminum.

For the first problem, our microscopic results for the loss spectrum of electrons backscattered from the Na/Al interface, reproduces the main features of data available, obtained with electron-energy loss spectroscopy. For alkali-metal coverages above one monolayer, the loss peak corresponding to a plasmon-like excitation, which grows from a broad structure for 1 monolayer to a sharp peak for two monolayers, while it shifts upward in energy. For coverages below one monolayer we obtain a broad structure between 0.5 and 1 monolayer, whose intensity depends of the incident electron energy ("ghost peak").

The behavior of the scattering probability for low coverages as a function of the incident energy, gives us a new mechanism to explain the different behavior of the dispersion of the loss peaks obtained at two experiments performed at different energies which show contrasting results.

In the second problem, we found longitudinal resonances on the three low index surfaces of aluminum. The surface resonance dispersion relations agree well with experimental data obtained with He-atom scattering performed on these surfaces. Comparing the experimental time-of-flight spectra with our calculated spectral densities of surface vibrations, we find a very good correspondence between the structures in the experiment and the spectral densities corresponding to displacements perpendicular to the surface. For the Al(110) surface we show the need of including multilayer relaxation in the calculation in order to obtain a sharp peak for the longitudinal resonance. A calculation performed with the unrelaxed surface, does not show this resonance. For the Al(100) and Al(111) surfaces, the resonances are weaker than for Al(110), and we attribute this to the fact that these surfaces relax very little. A study of the effect of the force constants on the resonances show that they are not related to a single force constant but to the total force field at the surface.

MICROSCOPIC STUDY OF ELECTRONIC SCREENING  
AT SIMPLE METAL SURFACES

by

Jorge Alberto Gaspar

A thesis submitted in partial fulfillment  
of the requirements for the degree

of

Doctor of Philosophy

in

Physics

MONTANA STATE UNIVERSITY  
Bozeman, Montana

February 1991

D378  
G2135

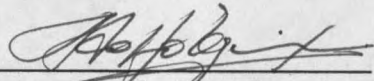
APPROVAL

of a thesis submitted by

Jorge Alberto Gaspar

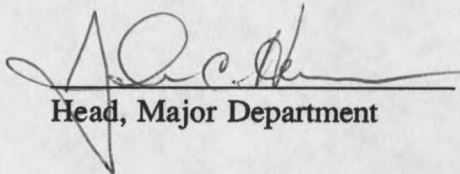
This thesis has been read by each member of the thesis committee and has been found to be satisfactory regarding content, English usage, format, citations, bibliographic style, and consistency, and is ready for submission to the College of Graduate Studies.

March 27, 1991  
Date

  
Chairperson, Graduate Committee

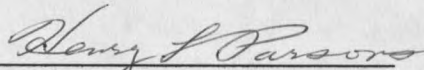
Approved for the Major Department

March 28, 1991  
Date

  
Head, Major Department

Approved for the College of Graduate Studies

April 4, 1991  
Date

  
Graduate Dean

## STATEMENT OF PERMISSION TO USE

In presenting this thesis in partial fulfillment of the requirements for a doctoral degree at Montana State University, I agree that the Library shall make it available to borrowers under rules of the Library. I further agree that copying of this thesis is allowable only for scholarly purposes, consistent with "fair use" as prescribed in the U.S. Copyright Law. Requests for extensive copying or reproduction of this thesis should be referred to University Microfilms International, 300 North Zeeb Road, Ann Arbor, Michigan 48106, to whom I have granted "the exclusive right to reproduce and distribute copies of the dissertation in and from microfilm and the right to reproduce and distribute by abstract in any format."

Signature

George Gaspar A.

Date

Feb. 26, 1991

## PUBLICATIONS BASED ON THE PRESENT WORK

"Microscopic Theory of Surface Phonons in Al(100): Mechanism for the Anomalous Behavior of the Dispersion Curves for Large Wave Vectors," J. A. Gaspar and A. G. Eguluz, *Phys. Rev. B (Rapid Comm.)* **40**, 11976 (1989).

"First-Principles Screening Calculation of the Surface Phonon Dispersion Curves at the (100) Surface of Sodium," A. Quong, A. A. Maradudin, R. F. Wallis, J. A. Gaspar, and A. G. Eguluz, in *Third Int. Conf. Phonon Physics*, edited by W. Ludwig (World Scientific, Singapore, 1990), p. 934.

"Theoretical Study of Surface Phonons and Resonances in Aluminum and its Comparison with Experiment," A. G. Eguluz, J. A. Gaspar, M. Gester, A. Lock, and J. P. Toennies, to appear in *Superlattices and Superstructures*.

"First-Principles Lattice Dynamics of the (100) Surface of Sodium," A. Quong, A. A. Maradudin, R. F. Wallis, J. A. Gaspar, A. G. Eguluz, and G. P. Alldredge, to appear in *Superlattices and Microstructures*.

"Dynamical Response of an Overlayer of Alkali-Metal Atoms Adsorbed on a Free-Electron Metal Surface," A. G. Eguluz and J. A. Gaspar, to appear in *Lectures in Surface Physics*, edited by M. Cardona and F. A. Ponce (Springer Verlag, Heidelberg).

"Elementary Excitations in an Overlayer of Alkali-Metal Atoms Probed by Electron Energy Loss Spectroscopy," J. A. Gaspar and A. G. Eguluz, Submitted to *Phys. Rev. Lett.*

"Resonances in the Surface-Phonon Spectrum of an sp-Bonded Metal," J. A. Gaspar, A. G. Eguluz, M. Gester, A. Lock, and J. P. Toennies, submitted to *Phys. Rev. Lett.*

"Transition from Two-Dimensional to Three-Dimensional Response in an Overlayer of Alkali-Metal Atoms: Breakdown of Macroscopic Physics," J. A. Gaspar, A. G. Eguluz, K. -D. Tsuei, and E. W. Plummer, in preparation.

"The Surface Lattice Dynamical Problem for Aluminum: Comparison Between First-Principles Calculation, Force-Constants Models, and Time-Flight Measurements," V. Bortolani, J. A. Gaspar, A. G. Eguluz, M. Gester, A. Lock, and J. P. Toennies, in preparation.

## TABLE OF CONTENTS

	Page
APPROVAL .....	ii
STATEMENT OF PERMISSION TO USE .....	iii
PUBLICATIONS BASED ON THE PRESENT WORK .....	iv
TABLE OF CONTENTS .....	v
LIST OF TABLES .....	vii
LIST OF FIGURES .....	viii
ABSTRACT .....	x
1. INTRODUCTION .....	1
2. THEORY OF ELECTRONIC SCREENING AT METAL SURFACES .....	9
Introduction .....	9
Local-Density-Functional Theory .....	9
Linear Response Method .....	11
Numerical Methods .....	13
3. SCATTERING PROBABILITY OF LOW ENERGY ELECTRONS FROM SIMPLE METAL SURFACES .....	18
Introduction .....	18
Electron-Energy-Loss Theory .....	19
Chemisorption Models .....	21
Loss Spectrum for Na/Al .....	23
4. MICROSCOPIC THEORY OF SURFACE PHONONS .....	48
Introduction .....	48
Microscopic Theory of Phonons .....	48
Bulk Phonons .....	49

## TABLE OF CONTENTS -Continued

Surface Phonons .....	53
Surface Phonons in Al(100): Mechanism for the Anomalous Behavior of the Dispersion Curves for Large Wave Vectors .....	57
Surface Phonons in Al(110) .....	64
Surface Phonons in Al(111) .....	76
Surface Resonances on Aluminum .....	79
5. CONCLUSIONS .....	91
REFERENCES .....	95

## LIST OF TABLES

Table	Page
1 Work function for Na/Al .....	23
2 Theoretical and experimental loss peaks as a function of coverage, for Na/Al. ....	31
3 Bulk phonon energies for aluminum .....	51
4 Bulk force constants for aluminum .....	53
5 Electronic and ionic contribution to some important surface force constants for Al(100) .....	61
6 Surface phonon energies at the $\bar{X}$ point for Al(110) .....	67
7 Surface phonon energies at the $\bar{Y}$ point for Al(110) .....	71
8 Surface force constants for Al(110) .....	73
9 Change of the Rayleigh phonon energy at the $\bar{X}$ point, for Al(110) surface, when some surface force constants are changed. ....	76

## LIST OF FIGURES

Figure	Page
1 Electronic density profile for Na/Al . . . . .	25
2 Surface energy-loss function for Na/Al . . . . .	27
3 Surface energy-loss function for 0.8 ML of Na/Al . . . . .	28
4 Energy-loss as a function of wave vector for 1.0 Na/Al . . . . .	29
5 Kinematic factor for $E_0=100$ eV, $\Theta=45^\circ$ . . . . .	30
6 Calculated loss spectrum for Na/Al for $E_0=100$ eV . . . . .	32
7 Calculated loss spectrum obtained for a macroscopic response model for Na/Al for $E_0=100$ eV . . . . .	33
8 Integrand of $I(\omega)$ for 0.6 ML . . . . .	36
9 $I(\omega)$ for $E_0=100$ eV and $E_0=30$ eV . . . . .	37
10 $I(\omega)$ for $E_0=100$ eV and 0.8 Na/Al for several aperture angles . . . . .	39
11 $I(\omega)$ for $E_0=30$ eV, several coverages . . . . .	40
12 Surface loss function for Na, computed for $q_{\parallel}=0.09 \text{ \AA}^{-1}$ . . . . .	42
13 Dispersion curves for the monopole and dipole surface plasmon of Na . . . . .	43
14 Dispersion curves for the surface plasmon and dipole surface plasmon for several coverages of Na/Al . . . . .	45
15 Dispersion curves for the surface plasmon and dipole surface plasmon for Sodium computed with LDA, Pseudo-RPA, and RPA . . . . .	46
16 Calculated phonon dispersion relation for bulk aluminum . . . . .	52
17 Pair potential for two ions in bulk aluminum . . . . .	55

## LIST OF FIGURES -Continued

Figure	Page
18 Pair potential for two ions at the Al(100) surface .....	56
19 Pair potential for two ions at the Al(110) surface .....	58
20 Surface-phonon dispersion relation curves for Al(100) .....	60
21 Dispersion relation for the RW along $\bar{\Gamma}-\bar{X}$ for Al(100) .....	65
22 Dispersion relation for the RW along $\bar{\Gamma}-\bar{M}$ for Al(100) .....	66
23 Surface-phonon dispersion relation curves for Al(110) computed with bulk FC's .....	68
24 Surface-phonon dispersion relation curves for the unrelaxed Al(110) surface .....	69
25 Surface-phonon dispersion relation curves for the relaxed Al(110) surface	70
26 Experimental TOF spectra for low index surfaces of Al, and calculated phonon spectral densities for Z-modes and L-modes .....	74
27 Longitudinal resonance and RW along $\bar{\Gamma}-\bar{X}$ on Al(110) .....	75
28 Spectral densities along $\bar{\Gamma}-\bar{X}$ on Al(100), for displacements perpendicular to the surface .....	77
29 Dispersion relation for the RW along four different directions in the surface Brillouin zone of the Al(111) surface .....	80
30 Spectral densities $\rho_{zz}$ computed along a scan curve .....	84
31 Scan curves along $\bar{\Gamma}-\bar{X}$ on the AL(110) surface .....	85
32 Longitudinal resonance and RW along $\bar{\Gamma}-\bar{X}$ on Al(110) computed with different FC's .....	87
33 Calculated dispersion curves for the RW and resonances for Z-modes and L-modes of the low index surface of Al .....	88
34 Spectral densities for $\bar{\Gamma}-\bar{X}$ direction of Al(110) along a scan curve ...	90

## ABSTRACT

We study electronic screening processes at simple metal surfaces. The jellium model is used for the ionic background of the metal. The linear electronic response of the metal is computed within the local density approximation of density functional theory. This theory is applied to two specific problems: 1) the electronic response of an alkali-metal overlayer chemisorbed on aluminum, and (2) the spectrum of surface vibrations of aluminum.

For the first problem, our microscopic results for the loss spectrum of electrons backscattered from the Na/Al interface, reproduces the main features of data available, obtained with electron-energy loss spectroscopy. For alkali-metal coverages above one monolayer, the loss peak corresponding to a plasmon-like excitation, which grows from a broad structure for 1 monolayer to a sharp peak for two monolayers, while it shifts upward in energy. For coverages below one monolayer we obtain a broad structure between 0.5 and 1 monolayer, whose intensity depends of the incident electron energy ("ghost peak").

The behavior of the scattering probability for low coverages as a function of the incident energy, gives us a new mechanism to explain the different behavior of the dispersion of the loss peaks obtained at two experiments performed at different energies which show contrasting results.

In the second problem, we found longitudinal resonances on the three low index surfaces of aluminum. The surface resonance dispersion relations agree well with experimental data obtained with He-atom scattering performed on these surfaces. Comparing the experimental time-of-flight spectra with our calculated spectral densities of surface vibrations, we find a very good correspondence between the structures in the experiment and the spectral densities corresponding to displacements perpendicular to the surface. For the Al(110) surface we show the need of including multilayer relaxation in the calculation in order to obtain a sharp peak for the longitudinal resonance. A calculation performed with the unrelaxed surface, does not show this resonance. For the Al(100) and Al(111) surfaces, the resonances are weaker than for Al(110), and we attribute this to the fact that these surfaces relax very little. A study of the effect of the force constants on the resonances show that they are not related to a single force constant but to the total force field at the surface.

## CHAPTER 1

### INTRODUCTION

Surface Physics is, because of its technological implications and its wealth of physical phenomena, a very active branch of Condensed Matter Physics. The very stringent experimental conditions required for the study of fundamental processes at surfaces have become more commonly obtainable in recent years. Many experimental techniques are now available for the study of the properties of solid surfaces, giving a diversified amount of information of the phenomena involved. We can mention as examples high resolution electron energy loss spectroscopy (HREELS),<sup>1</sup> helium-atom scattering spectroscopy,<sup>2</sup> photoemission spectroscopy (PS),<sup>3</sup> inverse photoemission spectroscopy (IPES),<sup>4</sup> scanning tunneling microscopy (STM),<sup>5</sup> etc.. By contrast, theory is well behind the sophistication of the experimental achievements. The main reason for this, is the very presence of the surface, which breaks translational symmetry in the direction normal to it. This breakdown increases the mathematical and computational complexity of the theory enormously in relation to the bulk. As a consequence, much of the theoretical work uses classical models for the response of the system, or transplants models from the bulk to the surface with some added boundary conditions, which dismisses valuable information about the surface which in most cases is the basis for the new physical processes

occurring there. After or during creation, the surface rearranges so as to lower its energy. This gives rise to new phenomena such as relaxation, reconstruction, surface states, etc., which have no counterpart in the bulk. Because of these changes, even a microscopic model that does not have some degree of self-consistency may not be appropriate for the study of surface processes.

The main challenge for the theory is thus to have a good enough modelling of the system under study and to be able to obtain its spectrum of elementary excitations, which will couple to external perturbations. In dealing with a system of  $10^{23}$  interacting particles, this is not an easy task, and many approximations are necessary before one is able to obtain any information about the system.

In the theory of solid surfaces, one must distinguish two stages which have evolved up to different levels of complexity and sophistication. The first stage is the study of the ground state properties of the system, which by now can be computed for all elements in the periodic table, obtaining total energies, and quantities related with it. The second stage (which is central to our work) refers to the response of surfaces to a perturbation. The importance of the knowledge of the response functions of the systems is related to the large amount of information contained in them (complementary to the ground state information), and because they are directly related with the measurement processes, i.e., the coupling between the elementary excitations of the system and external probes (electrons, atoms, photons, neutrons, etc.). Among the large variety of elementary excitations contained in the response functions, we can mention plasmons, phonons, excitons, magnons, etc.. The work on this issue is incipient and most existing studies use

the interacting free-electron gas model (pioneering for the bulk by Nozieres and Pines in the 50's<sup>6</sup>), in which a uniform positive charged background is used to replace the ions. The reason for this is clear: the inclusion of the lattice of ions into the problem makes the calculation extremely demanding from the point of view of the computational resources that are needed. Furthermore, even the calculation of bulk response functions is still to date a challenging problem, if the lattice of ions is taken into account.

A few papers devoted to the study of elementary excitations on semiconductor surfaces taking into account the lattice of ions have appeared recently,<sup>7</sup> but an efficient methodology for metals remains to be developed.

On the experimental side, there have been many recent studies, probing the spectrum of elementary excitations on simple metals surfaces. This is very convenient for a theorist, since the jellium model, within LDA, is best suited for simple metals.

The main purpose of this thesis is to compute, from first principles, several physical quantities in which electronic screening at simple metal surfaces plays a basic role. The unifying link in the problems discussed later is the central role played by  $\chi(\bar{x}, \bar{x}' | \omega)$  : the quantities of interest (scattering probability, total energy) are obtainable from a knowledge of this response function. The first step is to obtain the ground state density of the system, using the Kohn-Sham<sup>8</sup> set of self-consistent equations of density functional theory, within the local density approximation (LDA), and the jellium model. The electronic screening of the system is obtained from the density response function  $\chi(\bar{x}, \bar{x}' | \omega)$  which we compute (also within LDA) using the techniques developed in Refs. 9 and 10.

In the calculation of the different physical quantities using  $\chi(\bar{x}, \bar{x}' | \omega)$ , (surface phonons,<sup>11</sup> image plane position,<sup>12</sup>) the importance of the inclusion of exchange and correlation effects into the density response function has been demonstrated. Furthermore, these effects must be included consistently in the computation of both the ground state density and the density response function, in order that sum rules are obeyed.<sup>13</sup> The LDA density response function meets the just mentioned requirements. An extension of this theory for finite frequencies, based on an adiabatic ansatz for the exchange and correlation part of the effective electron-electron interaction, has been applied before with success to the study of the dynamical response of the loosely bound valence electrons of atoms, molecules and solid metals surfaces.<sup>14-16</sup>

Having outlined our framework, we specify two specific problems to which we have applied linear-response.

1.-A system which has attracted considerable attention for many years is that of overlayers of alkali-metal atoms chemisorbed on metal surfaces.<sup>16</sup> A major focus of this attention has been directed to the elucidation of the nature of the electronic excitations in the submonolayer and monolayer (ML) regimes.<sup>16-19</sup> Two new experiments have been performed recently on Na/Al(111),<sup>18,19</sup> aiming at an understanding of the physics of the adsorption and response of the overlayer at its simplest level, as one would expect for a system composed exclusively of *sp*-bonded metals. However, the results reported suggest qualitatively different response pictures. The high-resolution electron-energy-loss (EELS) experiment by Heskett *et al.*,<sup>19</sup> carried out at low incident energy  $E_0$ , identifies threshold coverage for plasmon formation to be about 1 ML. Below this threshold the observed loss

shifts downward in energy as the coverage is increased; the same is interpreted as a one-electron transition from the Na  $3s$ -level at the Fermi level into a coverage-dependent empty state. This assignment was supported by inverse-photoemission measurements.<sup>19</sup> A sharp discontinuity in the loss spectrum is observed for  $\sim 1$  ML. For coverage  $> 1$  ML the loss shifts upward with coverage, and is identified as an overlayer plasmon. By contrast, the loss spectrum of Hohlfeld and Horn,<sup>18</sup> obtained for high energy  $E_0$ , does not undergo a discontinuous jump for  $\sim 1$  ML. Starting from rather low coverage, their data show a broad peak, which initially occurs well below the surface plasmon frequency of Na. With increasing coverage the peak gains spectral weight in a monotonic fashion. For coverage  $> 1$  ML the loss is again interpreted as a plasmon.

The first purpose of our work on this problem, is to discuss the physics of the response in the ML-coverage regime, and its manifestation in an electron energy-loss experiment, via a self-consistent quantum mechanical calculation of the loss spectrum for an electron-gas model of the Na/Al system. For coverage  $< 1$  ML we find that the overlayer does not display coherent behavior, i.e. the loss function has no well-defined peak; however, the actual loss spectrum does show a peak whose spectral weight decays rapidly for low incident energy. As the coverage is increased past 1 ML the response of the electron gas becomes progressively more coherent (i.e., the loss function develops a peak), and the loss spectrum becomes a direct mapping of the spectral features of the overlayer response. The spectrum is then the same for all  $E_0$ . These results provide a means for bridging the gap between the two pictures of overlayer response suggested by the data of Refs. 18 and 19 for  $\sim 1$  ML.

We would like to note that our theoretical work on this problem was motivated by the experiments being conducted on Na/Al at Professor E. W. Plummer's laboratory at the University of Pennsylvania. As we will see in this thesis, our microscopic results give a good picture of the experimental results. On the other hand, a macroscopic model proves to be inadequate to interpret the experiment.

Another interesting result that we obtain for the Na/Al system is the theoretical determination of the existence of an additional surface plasmon in the overlayer for 2 ML coverage and above. As the coverage is increased, this mode becomes the multipole surface plasmon observed recently by Tsuei *et al.*<sup>16</sup>

2.- The second problem chosen for study is that of the dispersion relations of surface phonons and resonances at simple metal surfaces. Because of the complexity of the surface-screening problem, most of the theoretical work up to now has been reduced to the use of lattice-dynamical models, with use of FC's obtained by fitting to the bulk phonon frequencies.<sup>20-23</sup> However, these models are not unique in nature: for a given physical system there is more than one model capable of explaining the same data. It is only very recently that theoretical work using microscopic models has been reported.<sup>24-27</sup>

A proper treatment of surface vibrations needs to include the change of the force constants brought about by the presence of the surface in a self-consistent way. The density-response-method used in this thesis fulfills this requirement. As we will see later, the force constants are obtained from the computation of the pair potential between ions in the metal. The pair potential contains information about the presence of the surface, through the spatial dependence of the density response function. From the knowledge of

the FC's it is straightforward to obtain the dispersion relations for the surface phonons. Again, the basic ingredient in this method is the density response function  $\chi(x, x')$ .

Let us briefly outline some of the issues of interest in the field of surface phonons. The measured surface phonons dispersion relations for several surfaces show some features not explained by calculations performed with the use of bulk force constants. The most important of these differences, is the observation of anomalous surface-phonon resonances on the (111) and also the (110) surface of the noble metals<sup>28</sup> and several transition metals.<sup>29</sup> This has been a controversial issue because of the different ways in which the resonances have been explained.<sup>30,31</sup> The original argument suggests that the resonances are caused by a change in sp-d hybridization at the surface.<sup>30</sup> This explanation raises the question if the resonances are present for a simple metal such as aluminum. We have addressed this question in a recent collaboration with Professor J. P. Toennies' group at the Max-Planck Institut in Göttingen.<sup>32</sup> We have showed both experimentally and theoretically the existence of resonances at all three low-index surfaces of aluminum. We do not find a large softening of the radial surface FC, as has been proposed for noble metals<sup>30</sup>. Instead, we find that the resonances are produced by cumulative effects of changes in the entire surface force field.

At this point it is appropriate to comment on two other microscopic theories which have been developed for the calculation of surface phonon energies. One is the "direct method" implemented for aluminum by Ho and Bohnen,<sup>24</sup> for Na(110) by Rodach, Bohnen, and Ho<sup>33</sup> and for Au(110) by Lahee *et al.*<sup>34</sup> In this method, small distortions of the lattice are introduced and from total energy calculations, relevant elements of the

interplanar dynamical matrix are obtained. The power of the method is that it relies on state-of-the-art band-structure technology. Its main limitation is that, at the present time, it does not provide entire dispersion relations from first principles. The distortions necessary for the calculation of the dynamical matrix correspond to wave vectors at the center or the edge of the surface Brillouin zone. The other method is the so called "embedded atom" method,<sup>35</sup> in which the total energy of the solid is written in terms of a short-ranged pair potential between atoms and an embedding energy of each atom into the solid. By writing this embedding energy as a function of the superposition of the densities of all other atoms, one can obtain the FC's by differentiation. This method is phenomenological. The embedding energy as well as the pair potential are determined by fitting to bulk properties. Its main advantage is that it incorporates many-atom forces through the embedding energy function.

The outline of this thesis is the following. In Chapter 2 we recall the local-density-approximation (LDA) of density-functional theory, and outline the numerical method employed to obtain the response functions for a metal slab. In Chapter 3, we apply LDA to the problem of energy loss of electrons backscattered from metal surfaces, in particular, to the system Na/Al. A brief account is given of multipole plasmon excitations. In Chapter 4 we include the lattice of ions using pseudopotentials and perturbation theory for the determination of the surface phonons and resonances for the (100), (110), (111) surface of Al, and for Na(100). Finally in Chapter 5 we summarize our results, and highlight the main contributions of our work to the field of solid metal surfaces.

## CHAPTER 2

## THEORY OF ELECTRONIC SCREENING AT METAL SURFACES

Introduction

We begin this chapter by giving an account of the theory that constitutes the basic ingredients to this work. In the first section we briefly outline the standard method for the computation of the ground state electronic density of a solid, namely density-functional-theory, in the local-density-approximation (LDA).<sup>8</sup> In a subsequent section we describe the linear response method which gives us the induced electronic density produced by an external potential acting on a metallic system. Using density functional theory we obtain an integral equation for the density response function  $\chi(\vec{x}, \vec{x}')$ . Exchange and correlation effects are included within LDA. From the response function we obtain the induced density.

In the final section of this chapter, we define some quantities involved in the present work, and describe the method used to solve the integral equation for  $\chi(\vec{x}, \vec{x}')$ .

Local-Density-Functional Theory

The central theorem of density functional theory is due to Hohenberg and Kohn<sup>8</sup>, who showed that the ground state energy of an electronic system is a unique functional

of the ground state electronic density  $n_0(\vec{x})$ . Kohn and Sham<sup>8</sup> subsequently obtained a set of self-consistent equations which include exchange and correlation effects, and which make it possible to compute the ground state density of the system.

The set of self-consistent equations consists of a one-electron Schrödinger (Kohn-Sham) equation, namely

$$\left[-\frac{\hbar^2}{2m}\nabla^2 + V_{\text{eff}}(\vec{x})\right]\Psi_\nu(\vec{x}) = \epsilon_\nu \Psi_\nu(\vec{x}), \quad (2.1)$$

and the ground state density given, for  $T=0^\circ \text{K}$  by the equation

$$n_0(\vec{x}) = \sum_\nu f_\nu |\Psi_\nu(\vec{x})|^2, \quad (2.2)$$

where  $f_\nu = 2\Theta(E_F - \epsilon_\nu)$ ,  $E_F$  and  $\Theta(x)$  being the Fermi energy and the unit step function, respectively. The effective potential introduced in Eq. (2.1) is given by the equation

$$V_{\text{eff}}(\vec{x}) = v(\vec{x}) + \int d^3x' \frac{n_0(\vec{x}')}{|\vec{x} - \vec{x}'|} + V_{\text{xc}}(\vec{x}), \quad (2.3)$$

where  $v(\vec{x})$  is a static external potential, (for example, the ionic potential) and the so-called exchange and correlation potential  $V_{\text{xc}}(\vec{x})$  is defined by the equation

$$V_{\text{xc}}(\vec{x}) = \frac{\delta E_{\text{xc}}[n(\vec{x})]}{\delta n(\vec{x})}, \quad (2.4)$$

where we have introduced the exchange and correlation energy functional,  $E_{\text{xc}}[n]$ . The form of this functional for an inhomogeneous medium is unknown. The simplest possible ansatz, namely LDA, in which

$$E_{xc}[n] = \int d^3x n(\vec{x}) \epsilon_{xc}(n(\vec{x})) \quad (2.5)$$

$\epsilon_{xc}$  being the exchange and correlation energy per electron for an uniform electron gas of density  $n$ ,<sup>8,36</sup> turns out to be surprisingly successful.

The determination of the self-consistent ground state density, is reduced to the solution of the set of equations 2.1-2.2. Among the different approximations for  $\epsilon_{xc}$  we will use the Kohn-Sham approximation for the exchange potential reduced by a factor of 2/3 (equal to the local Slater approximation) and for the correlation potential we use the local Wigner interpolation approximation.<sup>8,36</sup>

With this prescription for  $V_{xc}$  we now have our set of equations fully determined and we need only to iterate through these equations until we obtain self-consistency. A numerical procedure to handle this problem has been given by Egiluz *et al.*<sup>36</sup>

### Linear Response Method

In this section we introduce the density response function, which is the basic ingredient for all the calculations performed in this work.

Consider our system with ground state density  $n_0(\vec{x})$  in the presence of an external perturbation  $U_{ext}(\vec{x})$ . The conduction electrons respond in such a way to this perturbation that an induced density  $n_{ind}(\vec{x})$  is set up in the solid, according to the equation

$$n_{ind}(\vec{x}) = \int d^3x' \chi^0(\vec{x}, \vec{x}') U_{sc}(\vec{x}'), \quad (2.6)$$

where we have introduced the static density response function for non-interacting

electrons,  $\chi^0(\vec{x}, \vec{x}')$ , defined by the equation<sup>36</sup>

$$\chi^0(\vec{x}, \vec{x}') = \sum_{v, v'} \left[ \frac{f_v - f_{v'}}{\epsilon_v - \epsilon_{v'}} \right] \Psi_v(\vec{x}') \Psi_{v'}^*(\vec{x}) \Psi_{v'}(\vec{x}') \Psi_v^*(\vec{x}), \quad (2.7)$$

The self-consistent potential  $U_{sc}(\vec{x})$  introduced in Eq. (2.6) is the sum of the external potential and the induced potential,  $U_{ind}(\vec{x})$ <sup>10</sup>. The self-consistent potential  $U_{sc}(\vec{x})$  is the total potential acting on the electrons as a consequence of the screening response of the electron system to the external field. In the LDA, we have

$$U_{ind}(\vec{x}) = e^2 \int d^3x' \frac{n_{ind}(\vec{x}')}{|\vec{x} - \vec{x}'|} + \frac{dV_{xc}(\vec{x})}{dn_0(\vec{x})} n_{ind}(\vec{x}). \quad (2.8)$$

where  $n_0(\vec{x})$ , denotes the electron number density in the ground state of the unperturbed system.  $U_{ind}(\vec{x})$  can be obtained from its definition as the change in the self-consistent potential  $V_{eff}(\vec{x})$  binding the electrons in the ground state.

Now, we can write the induced density,  $n_{ind}(\vec{x})$ , in terms of the external potential by the equation<sup>10</sup>

$$n_{ind}(\vec{x}') = \int d^3x \chi(\vec{x}, \vec{x}') U_{ext}(\vec{x}), \quad (2.9)$$

defining here the density response function  $\chi(\vec{x}, \vec{x}')$ .

It is straightforward to establish an integral equation for the density response function  $\chi(\vec{x}, \vec{x}')$ . Using symbolic notation we have that<sup>37</sup>

$$\begin{aligned}
n_{ind} &= \chi U_{ext} \\
&= \chi^{(0)}(U_{ext} + U_{ind}), \\
&= (\chi^{(0)} + \chi^{(0)}V\chi) U_{ext}.
\end{aligned}$$

Since the external potential is arbitrary, we must have that  $\chi = \chi^{(0)} + \chi^{(0)}V\chi$ , or using the full notation

$$\begin{aligned}
\chi(\vec{x}, \vec{x}') &= \chi^0(\vec{x}, \vec{x}') \\
&+ \int d^3x_1 \int d^3x_2 \chi^0(\vec{x}, \vec{x}_1) V(\vec{x}_1, \vec{x}_2) \chi(\vec{x}_2, \vec{x}'),
\end{aligned} \tag{2.10}$$

where the effective electron-electron interaction is given by

$$V(\vec{x}_1, \vec{x}_2) = \frac{e^2}{|\vec{x}_1 - \vec{x}_2|} + \frac{dV_{xc}(\vec{x})}{dn_0(\vec{x})} \delta(\vec{x}_1 - \vec{x}_2). \tag{2.11}$$

Equation 2.10 together with Eq. (2.9) are the keys to obtain a variety of physical observables related to the response of the system to an external perturbation. Although these equations are strictly valid only for the static case,  $\omega=0$ , an extension of them for finite frequencies using the same  $V_{xc}$  as for  $\omega=0$ , has been applied with success to atoms<sup>24,25</sup> and surfaces.<sup>38,39</sup>

### Numerical Methods

In this section we introduce several definitions that will be used throughout this work, and at the same time we give a brief description of the numerical procedures utilized to solve the ground state problem and the density response function.

Our basic approximation consists in the use of the jellium model, in which each layer of ions is replaced by a slab of uniform positive charge density, containing the same

amount of charge, and centered at the position of the original ions. The electronic charge distribution is then computed self-consistently by solving the set of Eqs. 2.1-2.2. A full description of a numerical method to obtain the self-consistent electronic profile has been given in Ref. 36.

We consider a metal slab containing  $N_L$  atomic layers. The total thickness of the jellium slab is given by  $bN_L$ ; its (number) density is denoted by  $\bar{n}_+$ . We take the  $z$  axis perpendicular to the surface. We suppose the electronic density actually vanishes at a distance  $z_0$  from the surface. The system is then confined between  $z=0$  and  $z=d$ , the jellium edges (uniform slab of positive charge) being located at  $z=z_0$  and  $d-z_0$ . The length  $z_0$  must be chosen to be sufficiently larger that its introduction does not perturb the physical observables we calculate beyond a given small tolerance.

Because of translational invariance on the plane of the surface (the plane  $xy$ ) for the jellium model, we can write the Kohn-Sham wave functions in the following form

$$\Psi_v(\vec{x}) = \frac{1}{A^{1/2}} e^{i\vec{k}_\parallel \cdot \vec{x}_\parallel} \phi_l(z), \quad (2.12)$$

where  $\vec{k}_\parallel$  and  $\vec{x}_\parallel$  are wave vector and position, respectively, in the plane of the surface, and  $A$  is the surface area. In this case the Kohn-Sham equation takes a one-dimensional form:

$$\left[ -\frac{\hbar^2}{2m} \frac{d^2}{dz^2} + V_{\text{eff}}(z) \right] \phi_l(z) = \varepsilon_l \phi_l(z), \quad (2.13)$$

where the energy eigenvalues  $\varepsilon_l$  are related to the eigenvalues  $E_v$  of the original equation,

(Eq. 2.1), according to

$$E_v = \frac{\hbar^2 k_{\parallel}^2}{2m} + \varepsilon_l, \quad l=1,2,3,\dots \quad (2.14)$$

In Eq. (2.13), the effective potential,  $V_{\text{eff}}$  is given by

$$V_{\text{eff}}(z) = -2\pi e^2 \int_0^d dz' [n_0(z') - n_+(z')] |z - z'| + V_{\text{xc}}(z), \quad (2.15)$$

where  $n_0(z)$  is the electronic density profile, and the density profile for the jellium slab is given by the equation

$$n_+(z) = \begin{cases} \bar{n}_+, & z_0 < z < d - z_0 \\ 0, & \text{otherwise.} \end{cases}$$

The wave functions  $\phi_l(z)$  are expanded in a Fourier sine series, according to the equation

$$\phi_l(z) = \left(\frac{2}{d}\right)^{1/2} \sum_{s=1}^{\text{smax}} a_s^{(l)} \sin\left(\frac{s\pi z}{d}\right). \quad (2.16)$$

Upon substitution of Eq. (2.16), and similar expansions for  $V_{\text{eff}}$  and  $n_0(z)$ , into Eq. (2.13), the differential equation reduces to a matrix equation for the coefficients  $a_s^{(l)}$ . We start the iteration of the self-consistency procedure with an initial guess for  $n_0(z)$ . For example, the next iteration step is always performed with a mixing of the old electronic density and the new one. In the calculation of the surface phonons for a 17 layers aluminum slab, a typical value for smax was 100.

The two-dimensional Fourier transform of the density response function is defined by the equation

$$\chi(\vec{x}, \vec{x}' | \omega) = \int \frac{d^2 k_{\parallel}}{(2\pi)^2} e^{i\vec{k}_{\parallel}(\vec{x}_1 - \vec{x}'_1)} \chi(k_{\parallel} \omega | z, z'). \quad (2.17)$$

Using similar Fourier representations for  $\chi^0$  and the effective electron-electron interaction,  $V(\vec{x}_1, \vec{x}_2)$ , in the Eq. 2.10, we obtain the following integral equation for the Fourier coefficients  $\chi(k_{\parallel} \omega | z, z')$

$$\begin{aligned} \chi(k_{\parallel} \omega | z, z') &= \chi^0(k_{\parallel} \omega | z, z') \\ &+ \int dz_1 \int dz_2 \chi^0(k_{\parallel} \omega | z, z_1) V(k_{\parallel} | z_1, z_2) \chi(k_{\parallel} \omega | z_2, z'), \end{aligned} \quad (2.18)$$

where the 2-dimensional Fourier transform of the effective electron-electron interaction is given by the equation

$$V(k_{\parallel} | z_1, z_2) = \frac{2\pi e^2}{k_{\parallel}} e^{-k_{\parallel}|z_1 - z_2|} + \frac{dV_{xc}(z_1)}{dn} \delta(z_1 - z_2). \quad (2.19)$$

The integral equation (2.18) was reduced to a matrix equation for the Fourier coefficients  $\chi_{mn}(k_{\parallel} \omega)$  through the introduction of a double-cosine Fourier representation for the density response function, noninteracting electron density response, and electron-electron interaction. The  $\chi_{mn}(k_{\parallel} \omega)$  are defined by

$$\chi(k_{\parallel} \omega | z, z') = \sum_{m=0}^{\infty} \sum_{n=0}^{\infty} \chi_{mn}(k_{\parallel} \omega) \cos\left(\frac{m\pi z}{d}\right) \cos\left(\frac{n\pi z'}{d}\right). \quad (2.20)$$

After the  $\chi_{mn}(k_{\parallel} \omega)$  are determined, we can compute the induced density in the system brought about by an external perturbation.

A detailed account of the numerical implementation of the above procedure is given in Ref. 10.

## CHAPTER 3

SCATTERING PROBABILITY OF LOW ENERGY ELECTRONS  
FROM SIMPLE METAL SURFACESIntroduction

In this chapter we study the electronic response of an alkali-metal overlayer adsorbed on aluminum (the system Na/Al). Since we will compare our theoretical results with relevant HREELS experiments, we begin with an outline of the theory for the inelastic backscattering of electrons from surfaces.

Next we outline the models of alkali-atom chemisorption we have employed in this work. The original uniform-background model of alkali-atom chemisorption provides a good overall account of the change in work function due to the adsorption process.<sup>39</sup> This model has recently been refined by Serena *et al.*<sup>40</sup> Both models are discussed below for coverages  $<$  one monolayer (saturation coverage). For coverages beyond one monolayer we resort to using a constant-density model.

Finally, we present our theoretical results for the loss spectrum for Na/Al, and compare them with experiment. We also discuss the dispersion relations for the surface plasmon and dipole-surface plasmon, for different coverages.

Electron-Energy-Loss Theory

A quantum-mechanical theory for the scattering of low energy electrons by surface excitations in the regime of small-angle deflections was given by Evans and Mills<sup>41,42</sup>. A simpler approach based on the model of a classical trajectory for the electrons impinging on the surface was later given by Schaich<sup>43</sup>. The later theory can be obtained from the quantum-mechanical theory after certain assumptions are made<sup>44</sup>. We will use here a hybrid model based on the classical trajectory for the incident electron, but which treats the response of the surface to the external perturbation produced by the incident electron quantum-mechanical. A recent review about electron scattering from surfaces, both theoretical and experimental is given in Ref. 1.

Consider an electron impinging on the surface at a time  $t=0$  and whose velocity is given by  $\vec{v}(t) = \vec{v}_{\parallel} - v_z \hat{z} \text{sgn}(t)$ , where  $\vec{v}_{\parallel}$  and  $v_z$  are the velocity components parallel and perpendicular to the surface respectively,  $\hat{z}$  is a unit vector perpendicular to the surface, and  $\text{sgn}(t) = +1(-1)$  if  $t > 0$  ( $t < 0$ ). The total energy lost by the electron during its interaction with the surface can be written in the form<sup>43</sup>

$$W = \int_0^{\infty} d\omega \hbar\omega I(\omega), \quad (3.1)$$

where  $I(\omega)$ , the probability per unit frequency that the electron has lost the energy  $\hbar\omega$ ,

is defined by the following equation

$$I(\omega) = \frac{2e^2 v^2}{\pi \hbar^2} \int_0^{\infty} \frac{d^2 q_{\parallel} P(q_{\parallel}; \omega)}{[v^2 q_{\parallel}^2 + (\omega - \vec{v}_{\parallel} \cdot \vec{q}_{\parallel})^2]^2} \quad (3.2)$$

In Eq. (3.2), we have introduced the surface energy-loss function  $P(q_{\parallel}; \omega)$ , which

is defined by the following equation

$$P(\vec{q}_{\parallel}; \omega) = -2\hbar e^2 \int_0^d dz \int_0^d dz' e^{-q_{\parallel}(z+z')} \text{Im} \chi(q_{\parallel}; \omega + i\eta | z, z'), \quad (3.3)$$

where  $\vec{q}_{\parallel}$  is the wave vector parallel to the surface, the length  $d$  is the spatial extent of the electronic system along the  $z$  axis, and  $\eta$  is a positive infinitesimal.

If both the substrate and overlayer are described by frequency-dependent dielectric functions  $\epsilon_b(\omega)$  and  $\epsilon_s(\omega)$ , respectively, the loss function is written as follows<sup>38</sup>

$$P(\vec{q}_{\parallel} | \omega) = \frac{2\hbar q_{\parallel}}{\pi} \text{Im} \frac{-1}{1 + \xi(q_{\parallel} | \omega)} \quad (3.4)$$

In Eq. (3.4) we have introduced the effective dielectric function of the adsorbate-substrate system,  $\xi(q_{\parallel} | \omega)$ , defined by the equation

$$\xi(q_{\parallel} | \omega) = \epsilon_s(\omega) \frac{1 + \Delta(\omega) e^{-2q_{\parallel} b}}{1 - \Delta(\omega) e^{-2q_{\parallel} b}} \quad (3.5)$$

where  $b$  is the thickness of the overlayer, and

$$\Delta(\omega) = \frac{\epsilon_b(\omega) - \epsilon_s(\omega)}{\epsilon_b(\omega) + \epsilon_s(\omega)}. \quad (3.6)$$

Note that for  $b=0$ , we have that  $\xi(q_{\parallel} | \omega) = \epsilon_b(\omega)$ , and the surface energy loss function  $P(q_{\parallel} | \omega)$  takes on the well-known form

$$P(q_{\parallel} | \omega) = \frac{2\hbar q_{\parallel}}{\pi} \text{Im} \frac{-1}{1 + \epsilon_b(\omega)} \quad (3.7)$$

which corresponds to an energy loss peak at the surface plasmon frequency of the substrate.

Now, because in the jellium model  $P(\vec{q}_{\parallel}; \omega)$  depends only on the magnitude and not on the direction of  $q_{\parallel}$ , Eq. (3.2) can be written as

$$I(\omega) = \frac{2e^2v^2}{\pi\hbar^2} \int_0^{q_{\max}} dq_{\parallel} K(q_{\parallel}; \omega) P(q_{\parallel}; \omega), \quad (3.8)$$

where  $q_{\max}$  is chosen to mimic the finite aperture angle of the spectrometer in the experiments. The kinematical factor  $K(q_{\parallel}; \omega)$  is given by

$$K(q_{\parallel}; \omega) = q_{\parallel} \int_0^{2\pi} d\theta \frac{1}{[v^2q_{\parallel}^2 + (\omega - v_{\parallel}q_{\parallel}\cos\theta)^2]}. \quad (3.9)$$

The analytic result for the angular integration in Eq. (3.9) has been given by Camley and Mills.<sup>44</sup> The value for  $q_{\max}$  is determined from the equation  $q_{\max} = k_{\perp} \Delta\theta$ , where  $\Delta\theta$  is the half width of the angular aperture of the spectrometer, and  $k_{\perp}$  the wave vector of the incident electron. In the following section we show results for the computation of  $I(\omega)$  for Na/Al and compare them with available experimental results from HREELS.

### Chemisorption Models

Before we start the study of the energy-loss spectrum, we describe the different models for alkali chemisorption within the framework of the jellium model. For coverages up to 1 ML we utilize the chemisorption model proposed by Serena *et al.*,<sup>40</sup> which is a variation of the original uniform-background model due to Lang.<sup>39</sup> The width  $d$  of the jellium slab for the adsorbate is given by

$$d(\theta) = d_{ion} + (b - d_{ion})\theta, \quad (3.10)$$

where  $\theta$  is the coverage,  $d_{ion}$  is twice the Na ionic radius, and  $b$  is the interplanar spacing for the (110) planes in the bulk. Monolayer coverage corresponds to  $\theta=1$  (for which the areal density of the overlayer is  $\sim 1/2$  that of an Al(111) substrate). While the use of  $d_{ion}$  in this model is not supported by new evidence for the absence of an ionic low-coverage regime,<sup>45,46</sup> the loss spectrum is rather insensitive to the details of the formula for  $d(\theta)$  for  $\theta < 1$ . The model does provide a very good account of the work function changes induced by alkali-atom adsorption. For  $\theta > 1$  we simulate the overlayer growth according to the equation  $d(\theta) = b\theta$ , which corresponds to keeping the density of the jellium slab for the second layer fixed; for  $\theta = 2$  the second layer is complete. With this choice, the work function remains equal to its saturation value; a variable-density model gives rise to a pronounced dip in the work function at the start of the second layer.

In Table 1 we show results for the work function as a function of coverage for the system Na/Al. For coverages beyond 1 ML it is observed experimentally that the work function remains close to the value for a thick alkali-metal slab. Although there have been some reports of a dip in the work function at the start of second layer<sup>18,47</sup> this is rather shallow. In using Lang's or Serena *et al.*<sup>40</sup> models to grow the second layer, one obtains a minimum for the work function comparable to that obtained for the first layer, which is in disagreement with the experiments reported until now. This suggests the use of a fixed density model to simulate the growth of the second layer. In this model the work function remains equal to its saturation value.

Table 1. Work Function (eV), for Na/Al. See text for explanation of the adsorption models.

Coverage $\theta$	Chemisorption Model		
	Fixed n	Lang	Serena <i>et al.</i>
0 (bare subst.)	3.8	3.8	3.8
0.5	-	2.49	2.58
0.7	-	2.82	2.81
0.8	-	2.94	2.93
1.0	3.10	3.10	3.10
1.25	3.17	2.18	2.51
1.50	3.12	2.61	2.74
1.75	3.05	2.88	2.93
2.0	3.06	3.06	3.06
Thick Na	3.09	-	-

#### Loss Spectrum for Na/Al

Most of the initial experiments of EELS on alkali-metal overlayers on metals, were performed with a noble or transition metal as substrate, reflecting the importance of these systems for technological applications. Very recently, experiments have been performed using aluminum as substrate. The absence of occupied d-bands in aluminum simplifies the physics involved. Furthermore the jellium model provides a good zeroth-order approximation. We should note that the motivation in using Al as substrate is the need

to understand the origin of the losses observed for coverages below 1 ML. The early experiments during the past years have been interpreted in terms of different mechanisms such as single-particle excitation<sup>48</sup>, transition from an occupied s-band to an unoccupied p-band<sup>19</sup>, transition from a substrate state to an unoccupied overlayer state<sup>49</sup>, and electron-hole pair excitation.<sup>38</sup>

In this section we show our theoretical results for the loss spectrum for different coverages of aluminum. We show first the ground state electronic-density for different coverages in Fig. 1. Results for clean aluminum is indicated as bare substrate, and the different coverages are given for each curve. From Fig. 1 we see that for 0.5 to 1 ML, the density profile does not show a bulk-like part while for 2 ML bulk-like plateau is already formed. This gives us a first hint of how inadequate it is to model the overlayer through the use of a bulk dielectric function that assumes a constant electronic density throughout the overlayer.

For this figure we have used an effective electron mass of 1.139 times the free electron mass, in order to fit the experimental value for the surface plasmon energy for Na of 4 eV. This produces a scaling of the peak positions. Also, we smoothed out the curves to eliminate background structure coming from the fact that we use a finite size for the substrate. Indeed, this could be eliminated also by increasing the value of the damping parameter. The value for  $\eta$  used in Eq. 3.6 is 0.05 eV which is ~1% of the plasma frequency for Sodium. A substrate thickness corresponding to 45 layers of Al(100) was used in the calculations, with  $s_{max}=120$ . It was checked that a larger basis gives essentially the same results.

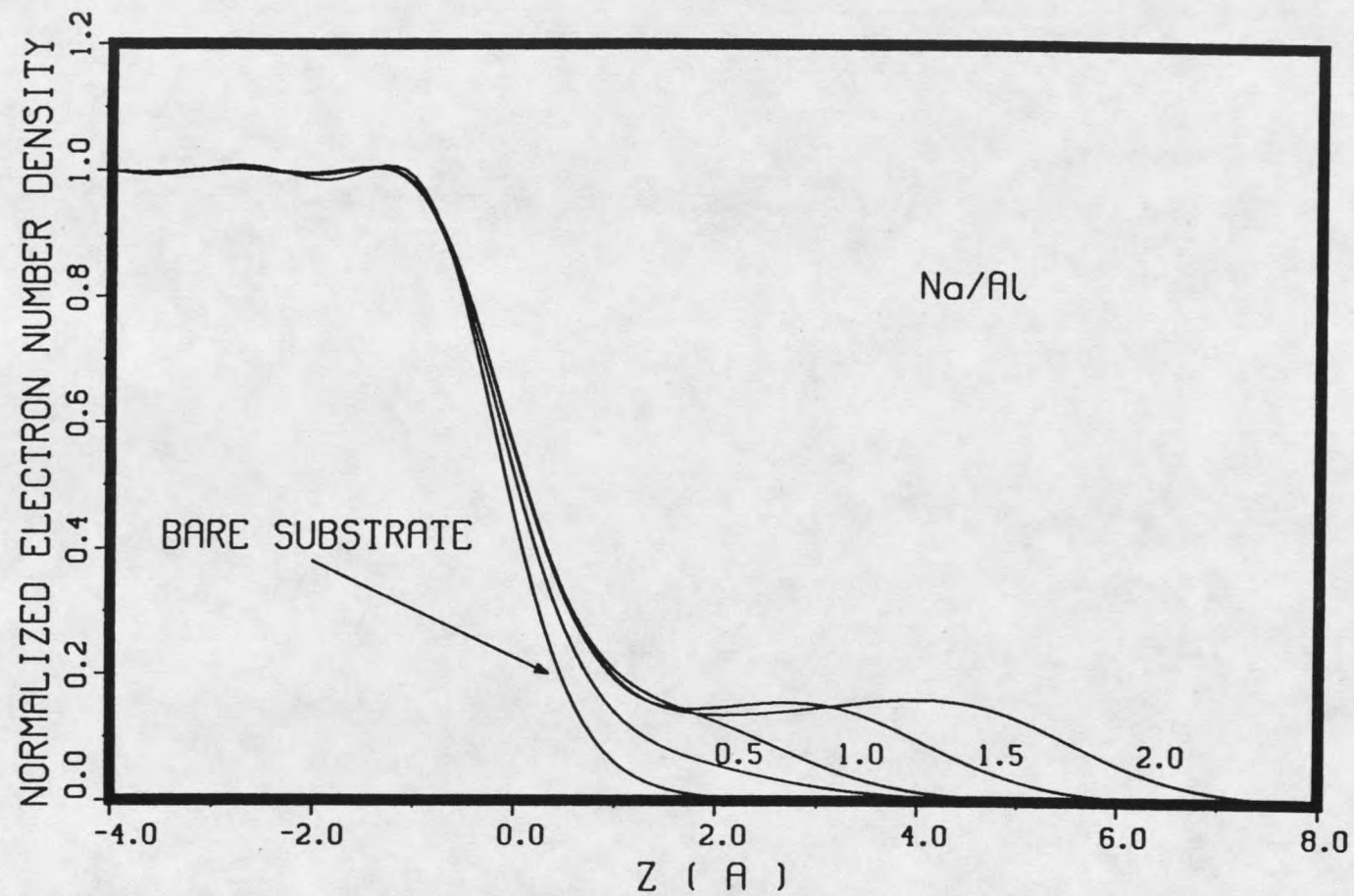


Fig. 1 - Electron number density profile for several coverages for the Na/Al system. Density number is normalized to the value for bulk aluminum. Coverages 1.0, 1.5, and 2.0 correspond to a fixed density model for chemisorption, while for 0.5 we have used Serena *et al*<sup>32</sup> model.

Figure 2 shows the loss function for several wave vectors, up to  $q_{\parallel\text{max}}$ . Clearly, for  $\theta < 1$  the overlayer response is featureless (except for its low energy drop-off); the same corresponds to incoherent electron hole pair excitation. As the coverage is increased the response gradually becomes coherent, and the loss function shows a peak. Collective mode-like peaks do not exist even for higher values of  $q_{\parallel}$  as shown by Eguiluz and Campbell,<sup>38</sup> and as can be appreciated in Fig. 3 for the wave vectors 0.11 and 0.13  $\text{\AA}^{-1}$  corresponding to 0.8 coverage. For an aperture angle of  $\sim 1^\circ$  and incident energies  $\leq 100$  eV, the values of  $q_{\parallel}$  which contribute to  $I(\omega)$  are  $< 0.1 \text{\AA}^{-1}$ . As one goes to coverages beyond 1 ML, a sharp structure corresponding to the surface plasmon begins to grow. The loss peak corresponding to the surface plasmon, as illustrated in Fig. 2 for  $\theta > 1.0$ , initially moves down in energy as a function of the wave vector.

In comparing the classical loss function (not shown) with the corresponding microscopic cases, we find that it represents a good approximation only for coverages close to or beyond two monolayers. For lower coverages, the SP peak in the classical case remains as sharp as for higher coverages, unlike the microscopic case. Moreover, the classical SP peak moves down in energy as a function of coverage from 1 ML to 2 ML.

The loss function is shown in Fig. 4 as a function of the wave vector, for different values of the frequency. This function, together with the kinematic factor,  $K(q_{\parallel}; \omega)$ , shown in Fig. 5 forms the integrand for  $I(\omega)$ . Although the loss function can have a rapidly varying structure as a function of  $\omega$ , it is a smooth function of  $q_{\parallel}$  for given  $\omega$ . Since  $K(q_{\parallel}; \omega)$  is also a smooth function of  $q_{\parallel}$ , the integration necessary to obtain  $I(\omega)$  is performed without difficulty.



















































































































































